Reversible, high-affinity surface capturing of proteins directed by supramolecular assembly

Di Palma, Giuseppe; Kotowska, Anna; Hart, Lewis; Scurr, David J.; Rawson, Frankie J.; Tommasone, Stefano; Mendes, Paula

DOI:
10.1021/acsami.9b00927

Reversible, high-affinity surface capturing of proteins directed by supramolecular assembly

Giuseppe Di Palma,[‡] Anna M. Kotowska,[§] Lewis R. Hart,[‡] David J. Scurr,[§] Frankie J. Rawson,[§] Stefano Tommasone,[‡] Paula M. Mendes[‡,*]

[‡]School of Chemical Engineering, University of Birmingham, Edgbaston, Birmingham, B15 2TT, UK.

Email: p.m.mendes@bham.ac.uk

[§]School of Pharmacy, University of Nottingham, Nottingham, NG7 2RD, UK.

KEYWORDS. Protein immobilization; supramolecular assembly; host-guest complexes; protein-surface interactions

ABSTRACT: The ability to design surfaces with reversible, high affinity protein binding sites represents a significant step forward in the advancement of analytical methods for diverse biochemical and biomedical applications. Herein, we report a dynamic supramolecular strategy to directly assemble proteins on surfaces based on multivalent host-guest interactions. The host-guest interactions are achieved by one-step nanofabrication of a well-oriented β-cyclodextrin host-derived self-assembled monolayer on gold (β-CD-SAM) that forms specific inclusion complexes with hydrophobic amino acids located on the protein's surface. Cytochrome C, insulin, α-chymotrypsin and RNase A are used as model guest proteins. Surface plasmon resonance (SPR) and static time of flight secondary ion mass spectrometry (ToF-SIMS) studies demonstrate that all four proteins interact with the β-CD-SAM in a specific manner via the hydrophobic amino acids on the surface of the protein. The β-CD-SAMs bind the proteins with high nanomolar to single-digit micromolar dissociation constants (K_D). Importantly, while the proteins can be captured with high affinity, their release from the surface can be achieved under very mild conditions. Our results expose the great advantages of using a supramolecular approach for controlling protein immobilization, in which the strategy described herein provides unprecedented opportunities to create advanced bioanalytic and biosensor technologies.

Keywords Supramolecular interactions; multivalent host-guest interactions; protein immobilization; cyclodextrins; self-assembled monolayers; surface plasmon resonance; time of flight secondary ion mass spectrometry

Introduction

Protein immobilization on material surfaces is at the heart of many biochemical and biomedical applications, ranging from development of biosensors,[1] bioanalytical tools,[2] to biocatalysis[3] and drug delivery.[4] Along with the widespread application of protein immobilization technology, there are also significant challenges to overcome and practical difficulties to resolve. Notably, proteins are required to be strongly linked onto the surface with high density without adversely affecting their activity.[5] Concomitantly, suitable immobilization methods are required that facilitate the facile release of the bound proteins to regenerate and reuse the assay, material or device.[6]

Over the years, many different approaches have been developed for tethering proteins to surfaces utilizing physisorption,[7] bioaffinity interaction[8] and covalent coupling.[9] Notable examples are the application of novel site-specific protein immobilization methods, which involve chemical or enzyme-mediated protein modification with chemical functionalities or bioaffinity ligands, followed by appropriate surface coupling.[10,11] The protein immobilization can be achieved either by using a variety of biorthogonal covalent crosslinking reactions to create a more permanent linkage[12] or by relying on reversible affinity-driven binding.[13] There are advantages and disadvantages to each of the aforementioned approaches, pertaining to simplicity of fabrication, reusability, stability of immobilized protein and retention of protein conformation and activity.[9,14]

A relatively unexplored strategy, although with vast potential, involves the use of non-covalent supramolecular interactions between proteins and supramolecular entities (e.g. cucurbituril, calixarenes and cyclodextrins).[15-21] Taking advantage of the highly stable chemistry of cucurbituril-ferrocene inclusion complexes, proteins have been site-specifically modified with ferrocene to be reversibly and stably immobilized onto a cucurbit[7]uril (CB[7]) monolayer.[22] In a recent example,[15] proteins have been tagged with a different number of hexahistidines (His6) at specific positions on the protein to understand its effect on protein orientation and binding strength upon interaction with nickel nitrilotriacetic acid (Ni-NTA) self-assembled monolayers. This strategy gave access to a high degree of control not only over the orientation of the pro-

teins on the surfaces but also to the binding strength of the proteins with the surface. Moreover the multivalency effect yielded dissociation constant values in the low nM regime. These and other examples in the literature[23-26] illustrate how supramolecular interactions and their predictability can be used to design protein immobilization systems with enhanced features and improved ability to tune their properties as required. Much though remains to be uncovered regarding the potential of supramolecular assembly for devising protein immobilization systems with emergent properties amenable to current needs. With this proviso in mind, in this work we investigated the ability of surface-tethered β-cyclodextrins (β-CDs) to promote facile, versatile and stable protein assembly but yet disassembly obviating the use of harsh conditions and protein denaturation.

CDs are macrocyclic oligosaccharide-derived non-symmetrical host molecules that selectively recognize, as a result of their apolar cone-shaped cavity, among other hydrophobic moieties, hydrophobic amino acids.[27] Notably, β-CDs have been demonstrated to form inclusion complexes with hydrophobic amino acids on the surfaces of proteins, namely phenylalanine (Phe), tyrosine (Tyr), leucine (Leu) and tryptophan (Trp).[27-31] These amino acids in the proteins can be strongly and selectively included into the β-CD cavity, forming complexes with mM binding affinity.[32] Furthermore, the interaction of β-CD moieties with proteins has been shown to inhibit protein unfolding, impart conformational protein stability and facilitate protein refolding.[32-35]

These capabilities have been used to good advantage in drug delivery[36] and formulation of pharmaceutical proteins.[37] However, there is clear scope to broaden the ways in which the unique β-CD-protein non-covalent interactions can be utilized to the modulation and assembly of proteins. In this framework, we present a study, enabled by the non-covalent interactions between β-CD and proteins, which demonstrates previously unmatched simplicity, versatility and capability to create highly stable, yet reversible, protein assemblies on material surfaces. Considering that proteins display at their surfaces multiple hydrophobic amino acids, we have harnessed the concept of multivalency[38] to promote the simultaneous binding of multiple amino acids on the protein to multiple well-oriented β-CD moieties tethered onto a gold surface. The heptathiolated derivative of β-CD (β-CD–(SH)7), in which the seven thiol moieties are installed on the smaller primary rim of the β-CD, was used to directly create a β-CD-terminated self-assembled monolayer (SAM) via multiple thiolate-gold covalent bonds (Scheme 1). This approach allows the larger secondary rim to be exposed at the interface, facilitating the binding of the amino acid residues from the protein surface inside the cavity. Four model proteins, namely cytochrome C, insulin, α-chymotrypsin and RNase A, which are distinct in structure and property and display randomly distributed hydrophobic amino acids throughout their surfaces (Figure 1) for β-CD binding, were investigated to assess the generality of our observations. The different hydrophobic amino acids on the surfaces of the proteins (i.e. Phe, Tyr, Leu and Trp) are also present at different densities (Table S1) thus further highlighting that the chosen four proteins can serve as general models for understanding protein-β-CD-SAM interactions.

Results and discussion

Since concentration and time play an important role on SAM formation and organization,[39,40] these parameters were investigated to evaluate the optimum conditions to create well-oriented surface tethered β-CDs. β-CD–(SH)7 SAMs were formed by immersing freshly cleaned gold substrates in either 0.1 mM or 1 mM DMF solutions of β-CD–(SH)7 for either 12, 24 or 48 h. In order to ascertain the properties of the formed β-CD–(SH)7 SAMs, contact angle, ellipsometry and X-ray photoelectron spectroscopy (XPS) analysis were carried out (Figure 2).

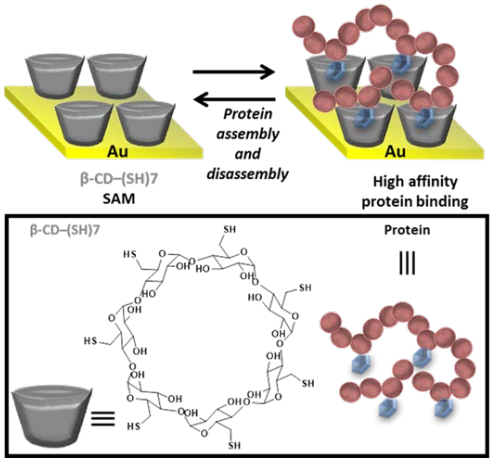

Scheme 1. Schematic representation of an effective supramolecular strategy to promote high and strong protein binding, which can be reversed under mild conditions. The strategy involves formation of a well-oriented β-CD–(SH)7 SAM, which forms multivalent interactions with hydrophobic moieties (shown as blue hexagons) present on the protein surface.

As illustrated by the water contact angle, all β-CD–

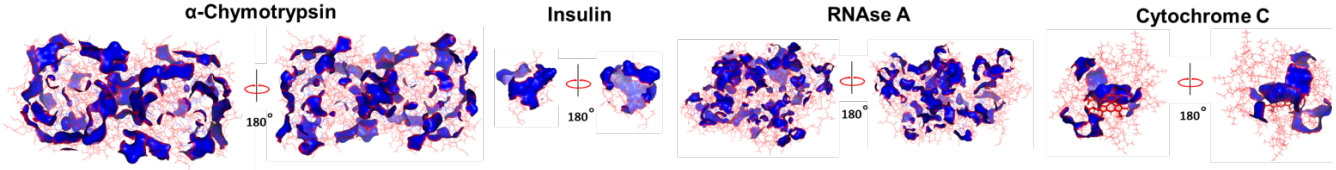

Figure 1. Overall structures of α-chymotrypsin, insulin, RNAse A and cytochrome C, with the hydrophobic amino acids on the surfaces of proteins (i.e. Phe, Tyr, Leu and Trp) highlighted in blue. The structural images were generated using PyMol.

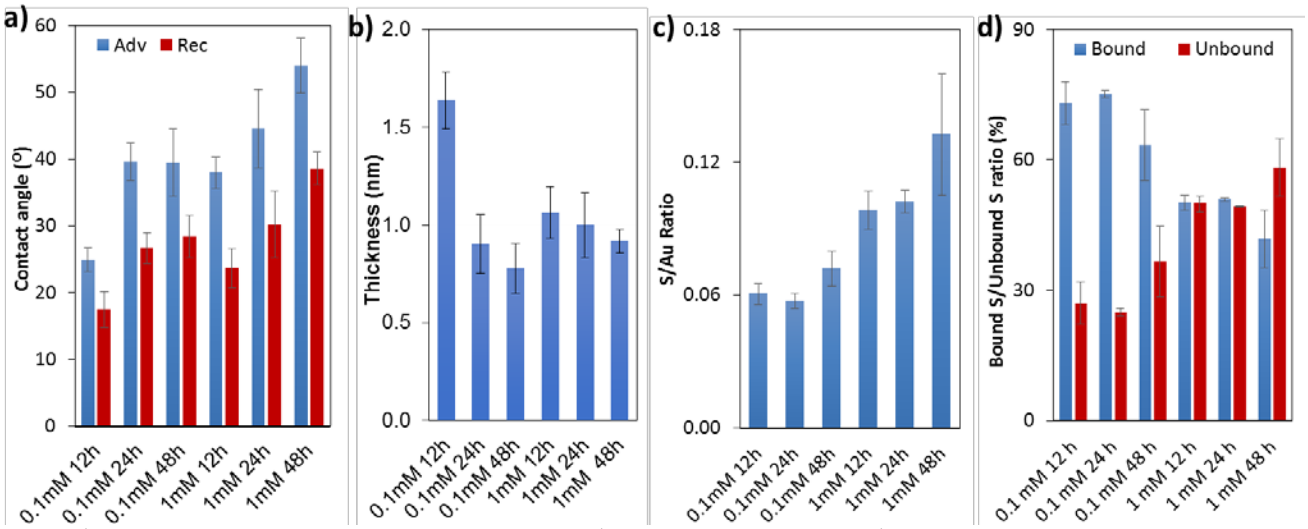

Figure 2. a) Advancing and receding water contact angles, b) ellipsometric thickness, c) S/Au ratio as determined by XPS analysis and d) Bound S/Unbound S ratio as determined by XPS analysis for the β-CD–(SH)7 SAMs formed using different concentrations and times. The error bars represent the standard deviation from either 9 (a and b) or 6 (c and d) measurements.

(SH)7 SAMs exhibit hydrophilic properties (Figure 2a) due to the presence of the hydroxyl groups on the outer edge of the amphiphilic β-CD molecules. However, their hydrophilicity differs, with advancing contact angle ranging from 25° (0.1 mM-12 h) to 55° (1 mM-48 h). These differences in hydrophilicity can provide some indication of the orientation of the CD macrocycle on the surface, where a decrease in hydrophilicity of the SAM might suggest the presence of a more exposed hydrophobic cavity at the interface. While significant contact angle differences were observed between 0.1 mM-12 h and 1 mM-48 h, the intermediate conditions show comparable advancing and receding contact angles. The hysteresis (θ_{Adv} - θ_{Rec}) values for all the β-CD–(SH)7 SAMs vary from 8° to 15°, suggesting the formation of relatively ordered and well defined monolayers.

Ellipsometry data (Figure 2b) provided further information regarding the organization of the SAMs, in which thickness dimensions close to the theoretical height of the β-CD molecule (0.78 nm)[41] were observed in all but one instance. This finding is consistent with the SAMs being packed with the C7 axis of β-CD orientated perpendicular to the plane of the gold surface. The SAM fabricated with a 0.1 mM solution of β-CD–(SH)7 incubated for 12 h exhibited a layer thickness of 1.60 nm, which is comparable to the theoretical outer diameter of the β-CD (1.54 nm).[41] This suggesting that the C7 axis of β-CD might be orientated parallel to the gold surface in this instance.

Further studies were carried out by XPS to probe the chemical composition and further understand the packing density of the SAMs. XPS data confirms the formation of the β-CD–(SH)7 SAMs, showing signals from the S (2p), O (1s) and C (1s) binding energies on all surfaces (data not shown). Interestingly, the ratios of S to Au (Figure 2c) and bound (S-Au) to unbound (SH) sulfur (Figure 2d) vary, depending mainly on the concentration used. The SAMs created by incubation of a 0.1 mM β-CD–(SH)7 solution exhibited a higher ratio of bound sulfur, even after only 12 h of incubation. The SAMs formulated with 0.1 mM solutions of β-CD–(SH)7 are attached to the surface via an average of 5 S-Au bonds, whereas 3-4 S-Au bonds are observed for the SAMs formed using 1 mM solutions of β-CD–(SH)7. As previously reported,[42] this difference in the number of covalent bonds formed can affect lateral diffusion during SAM formation and consequently surface molecular coverage. Indeed, the increased mobility restrictions imposed by the multiple thiol anchors associated with SAMs fabricated from 0.1 mM solutions could explain the lower sulfur content at these surfaces as established by calculating the XPS S/Au ratios. On the other hand, the higher sulfur content in SAMs formulated in a 1 mM solution provides an indication of a more tightly packed monolayer when compared with the SAMs formed from the 0.1 mM concentration. This characteristic is important for protein surface immobilization since sparsely packed CDs on the surface could lead to non-specific binding.

In order to further ascertain the density or permeability of the β-CD–(SH)7 SAMs, cyclic voltammetry (CV) studies were undertaken. Since β-CD moieties are known to form stable complexes with ferrocene and its derivatives,[43,44] water soluble ferrocene carboxylic acid (FCA) was used as a redox-active probe to quantify the β-CD surface density. β-CD–(SH)7 SAMs were immersed in a 0.1 M FCA solution for 4 hours and then rinsed with ultra-high quality (UHQ) water. Subsequently, the oxidation and the reduction potentials of FCA at the modified gold surfaces were investigated by cyclic voltammetry (Figure 3).

The cyclic voltammograms associated with surfaces modified with the 1 mM SAMs displayed the lowest anodic and cathodic current peak intensities. Interestingly the peak separation observed at CVs obtained for the 0.1 mM and 1 mM SAM-modified surfaces yielded peak separations of 41 ± 5 mV and 32 ± 3 mV, respectively. When peak separations fall below 59 mV, this is indicative of an elec-

trochemical surface bound process occurring.[45] This is further supported by the data in Figure S1, in which anodic peak currents obtained at varying scan rates are reported. Proportionality between peak current and scan rate indicated that ferrocene was bound to the surface. If it was under diffusion control however, proportionality to the square route of scan rate would be predicted, which was not observed. Interestingly, the higher concentration of CD found on SAMs fabricated from 1 mM solutions resulted in a lower peak separation, which is indicative of faster electron transfer kinetics *vs* the surface modified at lower concentrations.

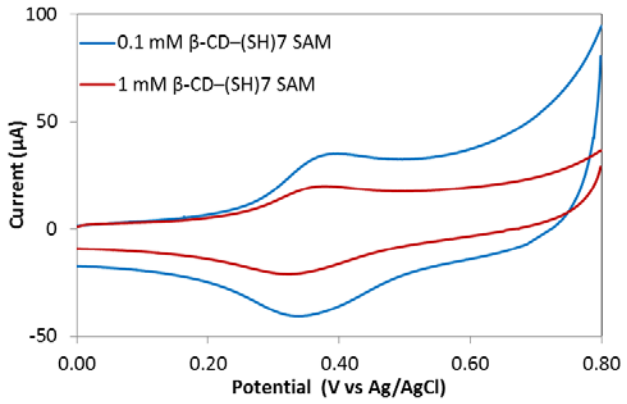

Figure 3. Typical cyclic voltammograms obtained in 0.2 M sodium sulfate solutions at a scan rate of 0.3 V/s of 0.1 mM β-CD–(SH)7 SAMs and 1 mM β-CD–(SH)7 SAMs, both formed for 24 hours. All the surfaces were exposed to a FCA solution for 4 hours.

Based on the CV data obtained for all different SAM conditions (*i.e.* varying concentration and incubation time), the surface coverages (Γ), as displayed in Figure 4, were determined according to the Laviron-derived equation for surface-confined electroactive species (Equation 1).[46]

$$\Gamma = \frac{I_p 4RT}{n^2 F^2 A \nu} \qquad (1)$$

Where I_p represents the peak current, R the gas constant, T the temperature, n the number of electrons in the Fe redox reaction (n=1), F the Faraday Constant, A the electroactive area (A= 0.785 cm^2) and ν the scan rate (ν = 0.3 V/s).

For reference purposes, the maximum theoretical ferrocene coverage (MTFC) on a CD SAM was also determined. By considering the 1:1 complexation between the CD and ferrocene in addition to the theoretical outer diameter of the β-CD (1.54 nm)[41] the MTFC was calculated to be 8.9 × 10^{-11} mol cm^{-2}. When comparing this theoretical value with the experimental values obtained for the 0.1 mM SAMs, it is evident that ferrocene interacts directly with the gold surface in addition to the CD modified SAM, thus increasing the overall current associated with the ferrocene electrochemistry. This behavior is likely to be a consequence of entrapment of ferrocene between the CD moieties indicated by the relatively larger peak separation.

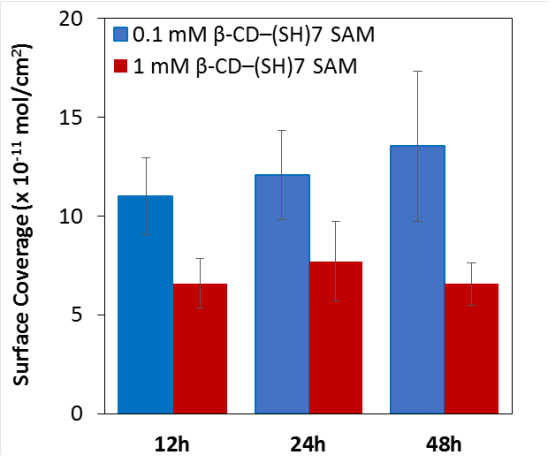

Figure 4. Ferrocene surface coverage obtained, as determined by CV analysis, for the β-CD–(SH)7 SAMs formed using different concentrations (0.1 mM and 1 mM) and times (12 h, 24 h and 48 h). The error bars represent the standard deviation from 3 measurements.

In cyclic voltammetry, the resultant current has two contributions. One is faradaic and another is capacitance

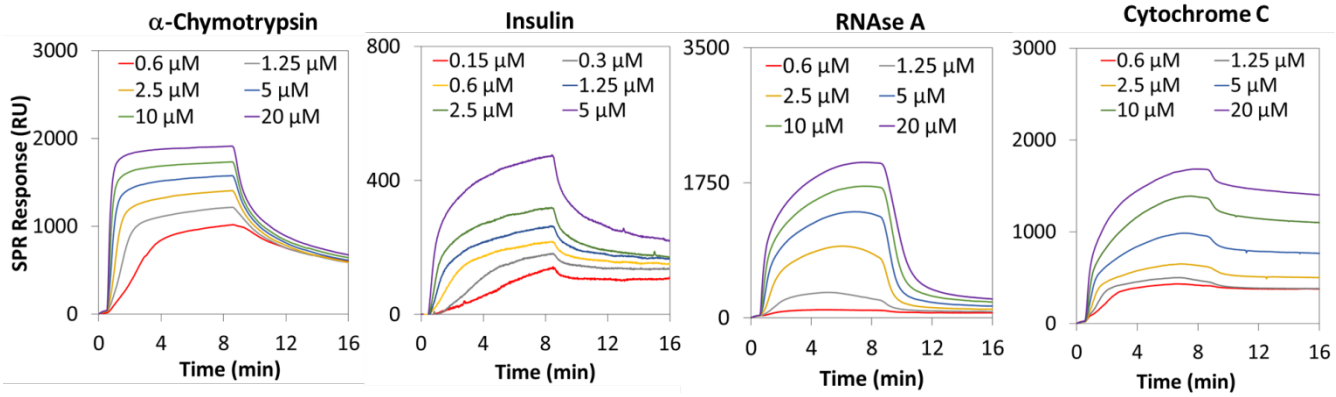

Figure 5. SPR sensorgram traces performed with 1 mM 24 h β-CD–(SH)7 SAMs and different concentrations of α-chymotrypsin, insulin, RNAse A and cytochrome C.

(charging currents). The charging current was larger (~16.2 μA at 0 V) for surface modified at the lower concentration of CD versus higher concentration (~8.0 μA at 0 V) as a result of lower packing density of the SAM. Therefore, ions can migrate to and from the electrode surface more readily in a given time, giving rise to the observed increase in charging current.[47-49] The data suggest that the 0.1 mM SAMs form loosely-packed structures, wherein the spaces between CDs are large enough for the ferrocene molecules to partake in electrochemical reaction at the bare gold surface. This results in a larger electrochemically active area which is revealed by the greater currents. In contrast, the SAMs formulated from 1 mM solutions display ferrocene surface coverages below but closer to the MTFC on a CD SAM, thus suggesting that ferrocene primarily complexes with the closely packed CD monolayer on the surface.

Each of the analytical techniques provided information regarding the packing and orientation of the CDs on the different β-CD–(SH)7 SAMs. Based on the hydrophilicity, the thickness of the monolayers and the number of bound thiols as determined by XPS, the CDs in both 0.1 mM and 1 mM SAMs are predominantly oriented with the macrocycle's cavity exposed at the interface. This orientation allows for maximum contact between the hydrophobic amino acid in the protein and the apolar CD cavity. However, the concentration used for SAM formation has an effect on the packing of the CDs on the gold surface. As highlighted by the reduced amount of S/Au ratio and increased permeability as demonstrated by cyclic voltammetry, SAMs fabricated with 0.1 mM solutions exhibited a less well packed structure of CDs. Thus, based on these findings, 1 mM SAMs incubated for 24 hours were chosen as the optimum surface to promote high protein binding while simultaneously limiting non-specific binding throught the presence of a packed CD surface.

Protein immobilization studies using surface plasmon resonance (SPR) spectroscopy demonstrated the assembly of the α-chymotrypsin, insulin, RNAse A and cytochrome C proteins on the β-CD–(SH)7 SAMs (Figure 5). Whilst the binding properties are somewhat dependent on the protein characteristics, all proteins bound to the CD functionalized surfaces with high nanomolar/low micromolar dissociation constants (K_D) as shown in Table 1.

The K_D values were calculated based on the SPR responses at equilibrium (R_{eq}), which were plotted against the concentration of injected protein (C_p) and fitted to a 1:1 steady-state affinity model. The model utilizes a non-linear least-squares regression method to fit data to the Langmuir adsorption isotherm (Equation 2). The equation not only allows calculating K_D but also the surface saturation response, R_{max}.

$$R_{eq} = \left(\frac{C_p}{C_p + K_D}\right) R_{max} \qquad (2)$$

Table 1. SPR-derived K_D values for the interaction between the 1 mM β-CD–(SH)7 SAM and the different proteins and protein binding capacity of the surface.

Protein	K_D **(μM)**	**Protein binding capacity (ng/nm²)**
α-Chymotrypsin	0.63 ± 0.20	1.93
Insulin	0.82 ± 0.35	0.55
RNAse A	1.12 ± 1.04	1.48
Cytochrome C	3.21 ± 0.90	1.78

The interaction between a single CD moiety and a hydrophobic binding site on the surface of a protein is weak, with K_D values typically in the mM range.[32] Thus, the recognition events occurring between the studied proteins and the CD–(SH)7 SAMs are characterized by multiple interactions acting simultaneously, affording more than 1000-fold increase in binding affinity. Chymotrypsin, insulin and RNAse A display, within the error, comparable binding affinities, while cytochrome C binds to the surface with the lowest affinity (K_D=3.21 μM). These finding are consistent with the surface percentage of hydrophobic amino acids on the four proteins as determined by PyMol (chymotrypsin, 19.0%; insulin 25.5%; RNAse A 19.9%; cytochrome C 15.6%). The lowest affinity obtained for cytochrome C might be correlated with the lowest surface percentage of hydrophobic amino acids in this protein. However, other parameters, which can possibly include type, orientation and accessibility of hydrophobic amino acids at the protein surface, might play a role in the overall affinity obtained.

It is, though, important to note that while the formation of the CD inclusion complexes with hydrophobic amino acids on the protein's surface has a large contribution to the SPR response and, thus binding affinity, other non-covalent interactions, such as hydrogen bonding, between the protein and the CD glucose units also play a role. This effect has been demonstrated by creating a gold-tethered SAM of glucose moieties as a control and conducting SPR spectroscopy analysis upon exposure to the different proteins. CDs are comprised of glucose monomers and thus the glucose-terminated SAM embodies similar functionalities at the interface but where the apolar cavity is not present. As shown in Figure S2, all the proteins bind to the glucose-terminated SAMs, however the SPR response is significantly lower than that seen for the β-CD–(SH)7 SAMs.

As anticipated, the SPR response for the β-CD–(SH)7 SAMs and the protein analytes are dependent on the protein molecular weight (M_w), with the lower M_w insulin displaying the lowest response. By considering R_{max} and that 100 response units (RUs) is equivalent to 0.1 ng/mm²,[50,51] the maximum protein binding capacity of the β-CD–(SH)7 SAM can be determined. As illustrated in Table 1, the β-CD–(SH)7 SAM possess a high capacity for

protein binding with protein densities ranging from *ca.* 0.5 ng/nm² to *ca.* 2 ng/nm², which are largely dependent on the protein M_w.

Moreover, as a result of the noncovalent nature of the CD–amino acid interactions, the captured proteins could be easily released from the surface by exposure to sodium dodecyl sulfate (SDS) (Figure 6). This "use-regenerate" cycle could be repeated multiple times with minimal loss of binding capability. Thus, reversibility of binding is clearly observed for the β-CD–(SH)7 SAM. However, bare gold surfaces, which are well-known for inducing random, non-biospecific protein adsorption,[52,53] were found to induce largely irreversible protein adsorption (Figure S3). These findings suggest[54] that on bare gold surfaces, the proteins might have undergone denaturation, ultimately attaching irreversibly to the surface.

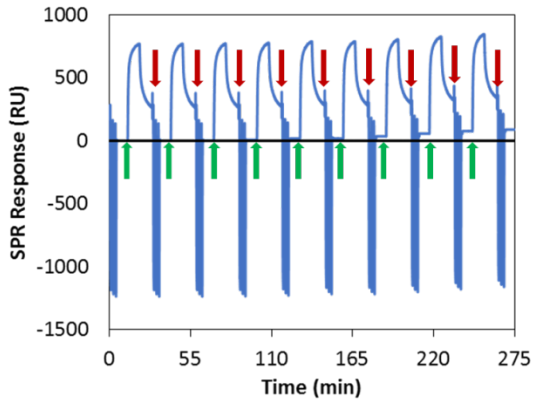

Figure 6. SPR responses from 9 SPR cycles that were performed using 2.5 μM α-chymotrypsin PBS solution on 1 mM 24 h β-CD–(SH)7 SAMs. The green arrows indicate the protein injection time and the red arrows show the beginning of the SDS regeneration step.

Time of flight secondary ion mass spectrometry (ToF-SIMS) studies were also conducted to understand whether the β-CD–(SH)7 SAM can induce a particular protein orientation on the surface. Static ToF-SIMS, which allows analysing the outermost 2 nm of the surface with high chemical specificity, has been previously used[55-57] to investigate the identity and orientation of surface-tethered proteins and a similar strategy was employed herein.

Cytochrome C, which contains a rigid porphyrin ring coordinated with a single iron atom, was used as the model protein to be studied by ToF-SIMS. The SAM fabricated by incubation of a 1 mM solution of β-CD–(SH)7 for 24 hours was exposed to a 1 mM cytochrome C solution in PBS for 2 hours, and subsequently rinsed in UHQ water. As a control, glucose-terminated SAMs were also exposed to similar cytochrome C incubation conditions. As further controls, ToF-SIMS analysis were also performed on bare gold and both β-CD–(SH)7 and glucose-terminated SAMs (Figure S4).

Since two types of chips: cytochrome C on glucose-terminated SAMs and cytochrome C on β-CD–(SH)7 SAMs have the same overall chemical composition, statistical analysis were required to identify more subtle differences between samples. Variance patterns within the ToF-SIMS secondary ion peak intensities between cytochrome C on the β-CD–(SH)7 SAM and the glucose-terminated SAM were analyzed by multivariate analysis in order to understand if differences in protein orientation could be inferred.[58,59] The ToF-SIMS relative ion intensities for cytochrome C on a β-CD–(SH)7 SAM and cytochrome C on a glucose-terminated SAM are significantly different from each other (Figure S5). To obtain more detailed information about protein orientation, the distinctive iron-porphyrin fragment ($C_{34}H_{33}N_4O_4Fe^+$, 617.27 m/z) of cytochrome C was examined on both protein surfaces (Figure 7a).

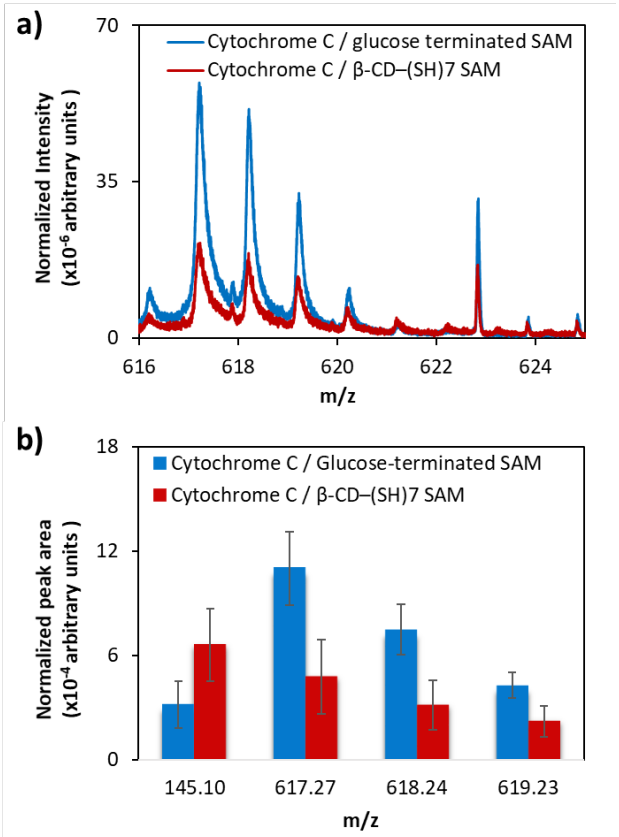

Figure 7. a) An overlay of the ToF-SIMS peak intensities and b) pattern peak intensities for cytrochrome C iron-porphyrin fragment, wherein the protein has been immobilized on either a glucose-terminated SAM or a β-CD–(SH)7 SAM. Peak areas are normalized to total ion count. Each bar shows peak area average of 12 measurements and standard deviation within sample set. Significance of differences between samples was confirmed by T-test.

The ion intensity of the iron-porphyrin (Mw = 618 Da) in both protein surfaces is remarkably different, with a lower ion intensity for the protein immobilized on the β-CD–(SH)7 functionalized SAM (Figure 7). As static ToF-SIMS collects chemical information from outermost 2 nm of the surface, these results indicate that on the β-CD–(SH)7 functionalized SAM, the cytochrome C prevalently adopts an orientation with the porphyrin ring pointing down towards the CD molecules and less available to the

primary ion beam. On the glucose-terminated SAMs, the cytochrome C porphyrin ring is more exposed to the analytical probe, resulting in a greater peak intensity. To support this hypothesis, other distinct fragments of cytochrome C were considered. The ion chosen was 145.10 m/z ($C_5H_9N_2O_3^+$), indicating the Gly1-Asp2 residue, which is located at the opposite side of the cytochrome C compared to the porphyrin ring. In this case, the trend in both protein surfaces is inverted, with a higher ion intensity for the protein immobilized on the β-CD–(SH)7 SAM (Figure 7b). These effects are not believed to have resulted from different protein amounts immobilized on the surfaces as although then overall peak intensities would change, normalized intensity patterns would be unaffected, as shown by Park *et al.*[58] This suggests that the interaction between the hydrophobic amino acids and the CD cavities in the β-CD–(SH)7 functionalized SAM are capable of inducing a defined protein orientation, which is different from that induced by other non-covalent interactions. There is the likelihood that this orientation is dictated by the position of the hydrophobic amino acids on the protein surface that can form stronger interactions with the surface-tethered CDs.

Conclusions

Herein, a surface molecular design was devised and developed that harnessed supramolecular chemistry to enable, for the first time, the construction of reversible, high-affinity protein assemblies on material surfaces solely through tailor-designed non-covalent interfaces. The facile approach does not require any protein modification process. While this study used gold-thiol SAMs, the methodology is sufficiently flexible to be applied to other substrate geometries (e.g. nanoparticles) and chemistries. Even though the exact binding properties and orientation of the protein on the CD-modified surface will always be dictated by the protein structure (i.e. unique distribution of hydrophobic groups on the surface of proteins), the strategy can be applied to a wide range of proteins, immobilize single or multiple proteins and provide high nanomolar to low micromolar dissociation constants. Additionally, while the proteins are tightly bound to the surface due to specific formation of inclusion complexes and multivalency, the CD-terminated surfaces can be readily addressed to regenerate the free CDs. Moreover, the surface can be reused for protein immobilization post-regeneration. Considering all these attributes of broad applicability and versatility of CD-terminated surfaces to immobilize proteins, this work opens up unprecedented routes to develop advanced bioanalytic platforms, in which the stable, reversible protein layer can act to efficiently promote the catch and release of target cells or other biological entities for downstream analysis.[60] Furthermore, the stability and recyclability associated with the new protein immobilization process provides a basis for meeting the demand to build re-usable biosensors and diagnostic devices.[61]

ASSOCIATED CONTENT

Supporting Information. Materials, methods and results on control surfaces. This material is available free of charge via the Internet at http://pubs.acs.org.

AUTHOR INFORMATION

Corresponding Author

* p.m.mendes@bham.ac.uk

Author Contributions

The manuscript was written through contributions of all authors. All authors have given approval to the final version of the manuscript.

Funding Sources

EPSRC (EP/K027263/1) and ERC (Consolidator Grant 614787).

ACKNOWLEDGMENT

The authors acknowledge financial support of this work by the EPSRC (EP/K027263/1) and ERC (Consolidator Grant 614787).

REFERENCES

(1) Samanta, D.; Sarkar, A. Immobilization of Bio-Macromolecules on Self-Assembled Monolayers: Methods and Sensor Applications. *Chem. Soc. Rev.* **2011**, 40, 2567-2592.

(2) Herr, A. E. Disruptive by Design: A perspective on engineering in analytical chemistry. *Anal. Chem.* **2013**, 85, 7622-7628.

(3) Britton, J.; Raston, C. L.; Weiss, G. A. Rapid Protein Immobilization for Thin Film Continuous Flow Biocatalysis. *Chem. Commun.* **2016**, 52, 10159-10162.

(4) Samanta, A.; Stuart, M. C. A.; Ravoo, B. J. Photoresponsive Capture and Release of Lectins in Multilamellar Complexes. *J. Am. Chem. Soc.* **2012**, 134, 19909-19914.

(5) Rusmini, F.; Zhong, Z. Y.; Feijen, J. Protein Immobilization Strategies for Protein Biochips. *Biomacromolecules* **2007**, 8, 1775-1789.

(6) Fraas, R.; Franzreb, M. Reversible Covalent Enzyme Immobilization Methods for Reuse of Carriers. *Biocatal. Biotransformation* **2017**, 35, 337-348.

(7) Yakovleva, J.; Davidsson, R.; Lobanova, A.; Bengtsson, M.; Eremin, S. A.; Laurell, T.; Emneus, J. Microfluidic Enzyme Immunoassay Using Silicon Microchip with Immobilized Antibodies and Chemiluminescence Detection. *Anal. Chem.* **2002**, 74, 2994-3004.

(8) Jung, Y.; Jeong, J. Y.; Chung, B. H. Recent Advances in Immobilization Methods of Antibodies on Solid Supports. *Analyst* **2008**, 133, 697-701.

(9) Wong, L. S.; Khan, F.; Micklefield, J. Selective Covalent Protein Immobilization: Strategies and Applications. *Chem. Rev.* **2009**, 109, 4025-4053.

(10) Ott, W.; Durner, E.; Gaub, H. E. Enzyme-Mediated, Site-Specific Protein Coupling Strategies for Surface-Based Binding Assays. *Angew. Chem.-Int. Edit.* **2018**, 57, 12666-12669.

(11) Zhang, Y.; Park, K. Y.; Suazo, K. F.; Distefano, M. D. Recent progress in enzymatic protein labelling techniques and their applications. *Chem. Soc. Rev.* **2018**, 47, 9106-9136.
(12) Chen, Y. X.; Triola, G.; Waldmann, H. Bioorthogonal Chemistry for Site-Specific Labeling and Surface Immobilization of Proteins. **2011**, 44, 762-773.
(13) Eva, B.; Blanka, K.: Affinity Interactions as a Tool for Protein Immobilization. In *Affinity Chromatography*; Magdeldin, S., Ed., 2012.
(14) Pascal, J.; Dirk, W.; Hendrik, S.; M., N. C.; Herbert, W. Chemical Strategies for Generating Protein Biochips. *Angew. Chem. Int. Ed.* **2008**, 47, 9618-9647.
(15) Wasserberg, D.; Cabanas-Danes, J.; Prangsma, J.; O'Mahony, S.; Cazade, P. A.; Tromp, E.; Blum, C.; Thompson, D.; Huskens, J.; Subramaniam, V.; Jonkheijm, P. Controlling Protein Surface Orientation by Strategic Placement of Oligo-Histidine Tags. *Acs Nano* **2017**, 11, 9068-9083.
(16) Wasserberg, D.; Cabanas-Danes, J.; Subramaniam, V.; Huskens, J.; Jonkheijm, P. Orthogonal Supramolecular Protein Assembly on Patterned Bifunctional Surfaces. *Chem. Commun.* **2018**, 54, 1615-1618.
(17) Weineisen, N. L.; Hommersom, C. A.; Voskuhl, J.; Sankaran, S.; Depauw, A. M. A.; Katsonis, N.; Jonkheijm, P.; Cornelissen, J. Photoresponsive, Reversible Immobilization of Virus Particles on Supramolecular Platforms. *Chem. Commun.* **2017**, 53, 1896-1899.
(18) Zhan, W.; Wei, T.; Yu, Q.; Chen, H. Fabrication of Supramolecular Bioactive Surfaces via β-Cyclodextrin-Based Host–Guest Interactions. *ACS Appl. Mater. Interfaces* **2018**, 10, 36585-36601.
(19) Zhan, W.; Wei, T.; Cao, L.; Hu, C.; Qu, Y.; Yu, Q.; Chen, H. Supramolecular Platform with Switchable Multivalent Affinity: Photo-Reversible Capture and Release of Bacteria. *ACS Appl. Mater. Interfaces* **2017**, 9, 3505-3513.
(20) Rennie, M. L.; Fox, G. C.; Perez, J.; Crowley, P. B. Auto-regulated Protein Assembly on a Supramolecular Scaffold. *Angew. Chem.-Int. Edit.* **2018**, 57, 13764-13769.
(21) Li, W.; Bockus, A. T.; Vinciguerra, B.; Isaacs, L.; Urbach, A. R. Predictive recognition of native proteins by cucurbit 7 uril in a complex mixture. *Chem. Commun.* **2016**, 52, 8537-8540.
(22) Young, J. F.; Nguyen, H. D.; Yang, L. T.; Huskens, J.; Jonkheijm, P.; Brunsveld, L. Strong and Reversible Monovalent Supramolecular Protein Immobilization. *Chembiochem* **2010**, 11, 180-183.
(23) Wasserberg, D.; Nicosia, C.; Tromp, E. E.; Subramaniam, V.; Huskens, J.; Jonkheijm, P. Oriented Protein Immobilization using Covalent and Noncovalent Chemistry on a Thiol-Reactive Self-Reporting Surface. *J. Amer. Chem. Soc.* **2013**, 135, 3104-3111.
(24) Gonzalez-Campo, A.; Brasch, M.; Uhlenheuer, D. A.; Gomez-Casado, A.; Yang, L. T.; Brunsveld, L.; Huskens, J.; Jonkheijm, P. Supramolecularly Oriented Immobilization of Proteins Using Cucurbit 8 uril. *Langmuir* **2012**, 28, 16364-16371.
(25) Lee, Y.; Lee, E. K.; Cho, Y. W.; Matsui, T.; Kang, I. C.; Kim, T. S.; Han, M. H. Proteochip: A Highly Sensitive Protein Microarray Prepared by a Novel Method of Protein, Immobilization for Application of Protein-Protein Interaction Studies. *Proteomics* **2003**, 3, 2289-2304.
(26) Qu, Y.; Wei, T.; Zhan, W.; Hu, C.; Cao, L.; Yu, Q.; Chen, H. A Reusable Supramolecular Platform for the Specific Capture and Release of Proteins and Bacteria. *J. Mater. Chem. B* **2017**, 5, 444-453.
(27) Aachmann, F. L.; Otzen, D. E.; Larsen, K. L.; Wimmer, R. Structural Background of Cyclodextrin-Protein Interactions. *Protein Eng.* **2003**, 16, 905-912.
(28) Otzen, D. E.; Knudsen, B. R.; Aachmann, F.; Larsen, K. L.; Wimmer, R. Structural Basis for Cyclodextrins' Suppression of Human Growth Hormone Aggregation. *Protein Sci.* **2002**, 11, 1779-1787.
(29) Dotsikas, Y.; Loukas, Y. L. Kinetic Degradation Study of Insulin Complexed with Methyl-Beta Cyclodextrin. Confirmation of Complexation with Electrospray Mass Spectrometry and H-1 Nmr. *J. Pharm. Biomed. Anal.* **2002**, 29, 487-494.
(30) Horsky, J.; Pitha, J. Inclusion Complexes of Proteins - Interaction of Cyclodextrins with Peptides Containing Aromatic-Amino-Acids Studied by Competitive Spectrophotometry. *J. Incl. Phenom. Mol. Recogn. Chem.* **1994**, 18, 291-300.
(31) Khajehpour, M.; Troxler, T.; Nanda, V.; Vanderkooi, J. M. Melittin as Model System for Probing Interactions Between Proteins and Cyclodextrins. *Proteins* **2004**, 55, 275-287.
(32) Serno, T.; Geidobler, R.; Winter, G. Protein Stabilization by Cyclodextrins in the Liquid and Dried State. *Adv. Drug Deliv. Rev.* **2011**, 63, 1086-1106.
(33) Ghosh, S.; Ghosh, C.; Nandi, S.; Bhattacharyya, K. Unfolding and Refolding of a Protein by Cholesterol and Cyclodextrin: A Single Molecule Study. *Phys. Chem. Chem. Phys.* **2015**, 17, 8017-8027.
(34) Vandevenne, M.; Gaspard, G.; Belgsir, E. M.; Ramnath, M.; Cenatiempo, Y.; Marechal, D.; Dumoulin, M.; Frere, J. M.; Matagne, A.; Galleni, M.; Filee, P. Effects of Monopropanediamino-Beta-Cyclodextrin on the Denaturation Process of the Hybrid Protein BlaPChBD. *BBA Proteins Proteom.* **2011**, 1814, 1146-1153.
(35) Samra, H. S.; He, F.; Bhambhani, A.; Pipkin, J. D.; Zimmerer, R.; Joshi, S. B.; Middaugh, C. R. The Effects of Substituted Cyclodextrins on the Colloidal and Conformational Stability of Selected Proteins. *J. Pharm. Sci.* **2010**, 99, 2800-2818.
(36) Challa, R.; Ahuja, A.; Ali, J.; Khar, R. K. Cyclodextrins in Drug Delivery: An Updated Review. *AAPS PharmSciTech.* **2005**, 6, E329-E357.
(37) Varca, G. H. C.; Andreo, N.; Lopes, P. S.; Ferraz, H. G. Cyclodextrins: An Overview of the Complexation of Pharmaceutical Proteins. *Curr. Protein Pept. Sci.* **2010**, 11, 255-263.

(38) Badjic, J. D.; Nelson, A.; Cantrill, S. J.; Turnbull, W. B.; Stoddart, J. F. Multivalency and Cooperativity in Supramolecular Chemistry. *Accounts Chem. Res.* **2005**, 38, 723-732.
(39) Li, S.-S.; Xu, L.-P.; Wan, L.-J.; Wang, S.-T.; Jiang, L. Time-Dependent Organization and Wettability of Decanethiol Self-Assembled Monolayer on Au(111) Investigated with STM. *J. Phys. Chem. B.* **2006**, 110, 1794-1799.
(40) Campbell, G. A.; Mutharasan, R. Monitoring of the Self-Assembled Monolayer of 1-Hexadecanethiol on a Gold Surface at Nanomolar Concentration Using a Piezo-Excited Millimeter-Sized Cantilever Sensor. *Langmuir* **2005**, 21, 11568-11573.
(41) Sharma, N.; Baldi, A. Exploring Versatile Applications of Cyclodextrins: An Overview. *Drug Delivery* **2016**, 23, 739-757.
(42) Nelles, G.; Weisser, M.; Back, R.; Wohlfart, P.; Wenz, G.; Mittler-Neher, S. Controlled Orientation of Cyclodextrin Derivatives Immobilized on Gold Surfaces. *J. Am. Chem. Soc.* **1996**, 118, 5039-5046.
(43) Harada, A.; Takahashi, S. Preparation and Properties of Cyclodextrin-Ferrocene Inclusion Complexes. *J. Chem. Soc. Chem. Commun.* **1984**, 645-646.
(44) Rojas, M. T.; Koniger, R.; Stoddart, J. F.; Kaifer, A. E. Supported Monolayers Containing Preformed Binding-Sites - Synthesis And Interfacial Binding-Properties Of A Thiolated Beta-Cyclodextrin Derivative. *J. Am. Chem. Soc.* **1995**, 117, 336-343.
(45) Bard, A. J.; Faulkner, L. R.: *Electrochemical Methods: Fundamentals and Applications, 2nd Edition*; John Wiley & Sons, 2000.
(46) Laviron, E. General Expression of the Linear Potential Sweep Voltammogram in the Case of Diffusionless Electrochemical Systems. *J. Electroanal. Chem.* **1979**, 101, 19-28.
(47) Laredo, T.; Leitch, J.; Chen, M.; Burgess, I. J.; Dutcher, J. R.; Lipkowski, J. Measurement of the Charge Number Per Adsorbed Molecule and Packing Densities of Self-Assembled Long-Chain Monolayers of Thiols. *Langmuir* **2007**, 23, 6205-6211.
(48) Świetlow, A.; Skoog, M.; Johansson, G. Double-Layer Capacitance Measurements of Self-Assembled Layers on Gold Electrodes. **1992**, 4, 921-928.
(49) Luo, M.; Frechette, J. Electrochemical Stability of Low-Density Carboxylic Acid Terminated Monolayers. *J. Phys. Chem. C* **2010**, 114, 20167-20172.
(50) Lahiri, J.; Isaacs, L.; Tien, J.; Whitesides, G. M. A Strategy for the Generation of Surfaces Presenting Ligands for Studies of Binding Based on an Active Ester as a Common Reactive Intermediate: A Surface Plasmon Resonance Study. *Anal. Chem.* **1999**, 71, 777-790.
(51) Stenberg, E.; Persson, B.; Roos, H.; Urbaniczky, C. Quantitative-Determination of Surface Concentration of Protein with Surface-Plasmon Resonance Using Radiolabeled Proteins. *J. Colloid Interface Sci.* **1991**, 143, 513-526.
(52) Yoshimoto, K.; Nishio, M.; Sugasawa, H.; Nagasaki, Y. Direct Observation of Adsorption-Induced Inactivation of Antibody Fragments Surrounded by Mixed-PEG Layer on a Gold Surface. *J. Am. Chem. Soc.* **2010**, 132, 7982-7989.
(53) Caruso, F.; Furlong, D. N.; Kingshott, P. Characterization of Ferritin Adsorption onto Gold. *J. Colloid Interface Sci.* **1997**, 186, 129-140.
(54) Karlsson, M.; Ekeroth, J.; Elwing, H.; Carlsson, U. Reduction of Irreversible Protein Adsorption on Solid Surfaces by Protein Engineering for Increased Stability. *J. Biol. Chem.* **2005**, 280, 25558-25564.
(55) Wang, H.; Castner, D. G.; Ratner, B. D.; Jiang, S. Y. Probing the Orientation of Surface-Immobilized Immunoglobulin G by Time-Of-Flight Secondary Ion Mass Spectrometry. *Langmuir* **2004**, 20, 1877-1887.
(56) Wagner, M. S.; Castner, D. G. Analysis of Adsorbed Proteins by Static Time-Of-Flight Secondary Ion Mass Spectrometry. *Appl. Surf. Sci.* **2004**, 231, 366-376.
(57) Wagner, M. S.; Tyler, B. J.; Castner, D. G. Interpretation of Static Time-Of-Flight Secondary Ion Mass Spectra of Adsorbed Protein Films by Multivariate Pattern Recognition. *Anal. Chem.* **2002**, 74, 1824-1835.
(58) Park, J. W.; Cho, I. H.; Moon, D. W.; Paek, S. H.; Lee, T. G. ToF-SIMS and PCA of Surface-Immobilized Antibodies with Different Orientations. *Surf. Interface Anal.* **2011**, 43, 285-289.
(59) Trindade, G. F.; Abel, M.-L.; Watts, J. F. simsMVA: A Tool for Multivariate Analysis of ToF-SIMs Datasets. *Chemom. Intell. Lab. Syst.* **2018**, 182, 180-187.
(60) Liu, H. L.; Liu, X. L.; Meng, J. X.; Zhang, P. C.; Yang, G.; Su, B.; Sun, K.; Chen, L.; Han, D.; Wang, S. T.; Jiang, L. Hydrophobic Interaction-Mediated Capture and Release of Cancer Cells on Thermoresponsive Nanostructured Surfaces. *Adv. Mater.* **2013**, 25, 922-927.
(61) Gomes, B. S.; Simoes, B.; Mendes, P. M. The Increasing Dynamic, Functional Complexity of Bio-Interface Materials. *Nat. Rev. Chem.* **2018**, 2, 0120.

Table of Contents artwork